# Nuclear structure of $^{176}$Lu and its astrophysical consequences. II. $^{176}$Lu, a thermometer for stellar helium burning

N. Klay,* F. Käppeler, H. Beer, and G. Schatz
*Kernforschungszentrum Karlsruhe, Institut für Kernphysik, D-7500 Karlsruhe, Germany*
(Received 27 September 1990)

On the basis of the improved level scheme of $^{176}$Lu it is demonstrated that the stellar *s*-process production as well as the stellar beta decay rate of that nucleus depend strongly on temperature. This behavior results from the completely different half-lives of the ground state and the isomer; since these states are coupled by induced transitions in the hot stellar photon bath, the effective half-life of $^{176}$Lu is drastically reduced. The $5^-$ state at 838.64 keV was identified as the most efficient mediating level. Consequently, $^{176}$Lu can no longer be considered as a chronometer for the age of the *s* process; instead, it can be interpreted as an *s*-process thermometer yielding a temperature range between $2.4\times10^8$ to $3.6\times10^8$ K.

## I. INTRODUCTION

The long half-life of $41\times10^9$ yr [1] seemed to make $^{176}$Lu a particularly promising chronometer with respect to galactic history [2,3]. The fact that this isotope can be attributed unambiguously to the slow neutron capture process (*s* process) offers the possibility for a rather precise determination of the original $^{176}$Lu abundance, which could then be compared with the present abundance in the solar system for deriving an age of the *s*-process elements.

The *s*-process flow in the Yb-Lu-Hf region is sketched in Fig. 1; it follows the solid line due to neutron captures and subsequent beta decays when a short-lived nucleus is encountered. Abundance contributions from the *r* process are indicated by arrows according to the respective beta decay chains. Obviously, the *r*-process chain at mass 176 ends at stable $^{176}$Yb, leaving the *s* process as the only production mechanism for the isobars $^{176}$Lu and $^{176}$Hf (apart from minor *p*-process contributions). The classical approach for the *s* process could be used as an excellent tool for determining the original $^{176}$Lu abundance [4]. The only complication in interpreting $^{176}$Lu as an *s*-process chronometer seemed to be the existence of an isomeric state, which causes part of the *s*-process flow to bypass the long-lived ground state. This effect is considered in Fig. 1 by showing ground state and isomer separately. As indicated by the strength of the lines, neutron capture on $^{175}$Lu leads more frequently to the isomer, leaving only a small probability for the long-lived ground state.

This isomer decays exclusively to $^{176}$Hf with a half-life of only 3.68 h; this means that neutron captures feeding the isomeric state determine the original *s*-process abun-

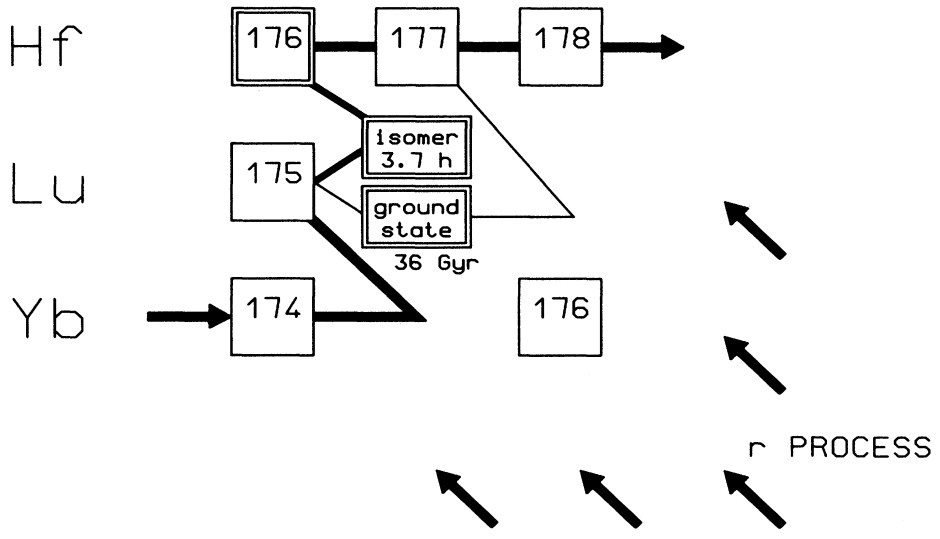


FIG. 1. The *s*-process neutron capture chain between Yb and Hf. For $^{176}$Lu, ground state and isomer are shown separately. Note that $^{176}$Lu and $^{176}$Hf are shielded against *r*-process beta decays.

 

dance of $^{176}$Hf. Such a picture, where the ground state and the isomer in $^{176}$Lu are treated as two different nuclei appeared plausible since direct electromagnetic $E6$ transitions between the $I^{\pi}=1^{-}$, $K=0$ isomer and the $I^{\pi}=7^{-}$, $K=7$ ground state are expected to be inhibited by selection rules. However, this straightforward interpretation was questioned by a number of problems. First, the partial capture cross section for populating the isomer in $^{176}$Lu was found to be much larger [5–8] than in a previous measurement [9], leading to a strongly reduced production of $^{176}$Lu that was even not sufficient to account for the observed abundance [10]. Secondly, Beer *et al.* [11] found in an extended analysis of the branching at $A=176$ that the effective $s$-process flow through $^{176}$Lu was considerably larger than expected from the partial neutron capture cross sections leading to the isomer and ground state, respectively.

Therefore, additional feeding mechanisms for the long-lived ground state had to be identified. The most important one was discussed as being due to the hot photon bath at the stellar $s$-process site [12,13]. Thermal photons may excite higher lying nuclear states which then decay back either to the isomer or to the ground state. In this way, the initial populations of these two states can be changed, and in the extreme case even thermal equilibrium can be achieved. Then, the $s$-process abundances of $^{176}$Lu and $^{176}$Hf no longer depend on partial neutron capture cross sections but on the competition between the stellar beta decay and neutron capture, resulting in an abundance ratio that is sensitive to temperature and neutron density during the $s$ process.

Experimental evidence for electromagnetic transformations between ground state and isomer was obtained by photoactivation of Lu samples in intense gamma-ray fields [14–16]. In these measurements, the isomer could be produced only with $^{60}$Co and $^{24}$Na sources but not with $^{137}$Cs, a hint that the mediating levels are at excitation energies above the 662 keV gamma-ray energy of $^{137}$Cs. However, quantitative information on the stellar transition rates could not be inferred from these measurements as the relevant properties of the mediating levels, i.e., their excitation energies and quantum numbers remained unknown.

An improved theoretical approach was presented by Gardner *et al.*[17] who complemented the experimentally determined levels in $^{176}$Lu by postulated states inferred from systematic trends in neighboring nuclei. With this "complete" level scheme it was possible to demonstrate that the temperature dependence of the $^{176}$Lu half-life could be obtained without violating the $K$-selection rule. This result underlines the importance of an experimental extension of the level scheme, which ultimately resolves the remaining uncertainties.

Another possible mechanism for exciting $^{176}$Lu is by positron annihilation with a $K$-shell electron [16,18]; however, the effect of this mechanism has probably been overestimated in the stellar plasma and may be important only at higher temperatures [19].

In paper I of this work (the preceding paper) the complete level scheme of $^{176}$Lu was established with the best experimental resolution and sensitivity up to excitation energies of $\sim$1 MeV, in order to identify the mediating levels for isomer and ground state. On this basis, the temperature effects on the $s$-process flow through the $A=176$ branching can now be treated quantitatively. The resulting astrophysical implications are discussed in the following.

## II. THE $s$-PROCESS BRANCHING AT $^{176}$Lu

### A. Definition of the branching factor

The calculation of the $^{176}$Lu abundance produced in the slow neutron capture process ($s$ process) must consider the branching in the neutron capture chain due to the comparably fast beta decay from the isomeric state. The $s$-process flow through $^{176}$Lu can be expressed by means of a branching factor $f_n$:

$$(\sigma N)_{^{176}\mathrm{Lu}}=f_n[(\sigma N)_{^{176}\mathrm{Lu}}+(\sigma N)_{^{176}\mathrm{Hf}}] \ . \tag{1}$$

Here, $\sigma N$ denotes the product of stellar neutron capture cross section $\sigma$ and the respective abundance produced by the $s$ process. As long as only the ground state decay of an unstable isotope is involved, the branching factor for this one-level system can be expressed by the ratio of the rates for neutron capture $\lambda_n$ and for beta decay $\lambda_\beta$:

$$f_n=\frac{\lambda_n}{\lambda_n+\lambda_\beta} \ . \tag{2}$$

If, in addition, excited states are involved, e.g., the isomer at 123 keV in $^{176}$Lu, Eq. (2) must be extended:

$$f_n=\frac{\Sigma n_j\lambda_n(i)}{\sum n_i[\lambda_n(i)+\lambda_\beta(i)]} \ , \tag{3}$$

where $n_i$ denotes the population of level $i$.

In case of $^{176}$Lu it is sufficient to consider beta decays and neutron captures from the ground state and the isomer. The many higher lying states may act as mediators for redistributing the initial populations of ground state and isomer, but they themselves are so weakly populated that their contributions to $\lambda_n$ and $\lambda_\beta$ can be neglected. Then, Eq. (3) simplifies to

$$f_n=\frac{n_g\lambda_n(g)+n_m\lambda_n(m)}{n_g[\lambda_n(g)+\lambda_\beta(g)]+n_m[\lambda_n(m)+\lambda_\beta(m)]} \ , \tag{4}$$

where the indices $g$ and $m$ refer to the ground state and to the isomer, respectively.

According to Eq. (4), the populations of ground state and isomer are decisive parameters for the determination of the branching factor $f_n$, which depend on the thermal coupling between ground state and isomer. A general time-dependent solution of this problem [20] was applied to $^{176}$Lu by Beer *et al.*[13] using Weisskopf estimates with constant retardation factors for the transition rates. Since the level scheme was incomplete at that time, only qualitative results could be obtained in this study.

With the complete level scheme derived in the present work, the calculation can now be restricted to the relevant energy levels. In this way, the branching factor can be given by an analytic approximation, thus avoiding

the numerical integration of the complex system of differential equations, which could be described only by global assumptions on the related transition rates, anyhow. The notation of Ward and Fowler [20] is largely used in the following discussion.

### B. Evolution of a three-level system to thermal equilibrium

Figure 2 shows a three-level system consisting of ground state, isomer, and a mediating level $i$. The evolution of this system to thermal equilibrium is followed first without considering the *external* production and destruction rates $\lambda_{p0}$, $\lambda_{0d}$, $\lambda_{pm}$, and $\lambda_{md}$. Changes of the initial population probabilities are to be expected if the time constant for approaching thermal equilibrium becomes comparable to the life times for beta decay or neutron capture. This time dependence of the population probabilities $n$ can be described by a system of differential equations:

$$\frac{dn_0}{dt}=-\rho B_{0i}n_0+(A_{i0}+\rho B_{i0})n_i \ , \tag{5a}$$

$$\frac{dn_i}{dt}=\rho B_{0i}n_0-(A_{i0}+\rho B_{i0})n_i-(A_{im}+\rho B_{im})n_i +\rho B_{mi}n_m \ , \tag{5b}$$

$$\frac{dn_m}{dt}=(A_{im}+\rho B_{im})n_i-\rho B_{mi}n_m \ . \tag{5c}$$

The transition probabilities between two levels 1,2 can be expressed in terms of the Einstein coefficients $A_{21}$, $B_{21}$ for emission, and $B_{12}$ for absorption, and of the radiation density $\rho$ that follows from the Planck formula. In thermal equilibrium, the Einstein coefficients are related by

$$\rho B_{12}=A_{21}\frac{g_2}{g_1}\frac{1}{\exp[(E_2-E_1)/kT]-1} \ , \tag{6a}$$

$$B_{21}=B_{12}g_1/g_2 \ , \tag{6b}$$

where $g_{1,2}=2I_{1,2}+1$ are the statistical factors according to the level spins $I$. These relations are not restricted to thermal equilibrium, but hold in general as long as the radiation density $\rho$ in the stellar plasma corresponds to a Planck distribution. Since the following discussion of thermal couplings between ground state and isomer in $^{176}$Lu always implies rather high photon energies $h\nu=\Delta E \gg kT$, stimulated emission can be neglected compared to spontaneous emission, and Eq. (6a) simplifies to

$$\rho B_{12}=A_{21}\frac{g_2}{g_1}\exp[-(E_2-E_1)/kT] \ . \tag{6c}$$

Solutions of Eqs. (5a)–(5c) can be obtained with the ansatz $n_x(t)=c_x\exp(\lambda t)$ with $x=0,m,i$. The time constants $\lambda$ are eigenvalues of the Eqs. (5a)–(5c) and are determined via the characteristic polynomial

$$\lambda[\lambda^2+\lambda(A_{i0}+A_{im})+\rho B_{0i}A_{im}+\rho B_{mi}A_{i0}]=0 \ . \tag{7}$$

with the nontrivial solutions

$$\lambda_{01}=-(A_{i0}+A_{im}) \ , \tag{8a}$$

$$\lambda_{02}=-\frac{\rho B_{mi}A_{i0}+\rho B_{0i}A_{im}}{A_{i0}+A_{im}} =-\frac{A_{i0}A_{im}}{A_{i0}+A_{im}}\frac{g_i}{g_m}\exp[-(E_i-E_m)/kT] \ . \tag{8b}$$

The first solution corresponds to the relatively quick relaxation of the system if the population of the mediating

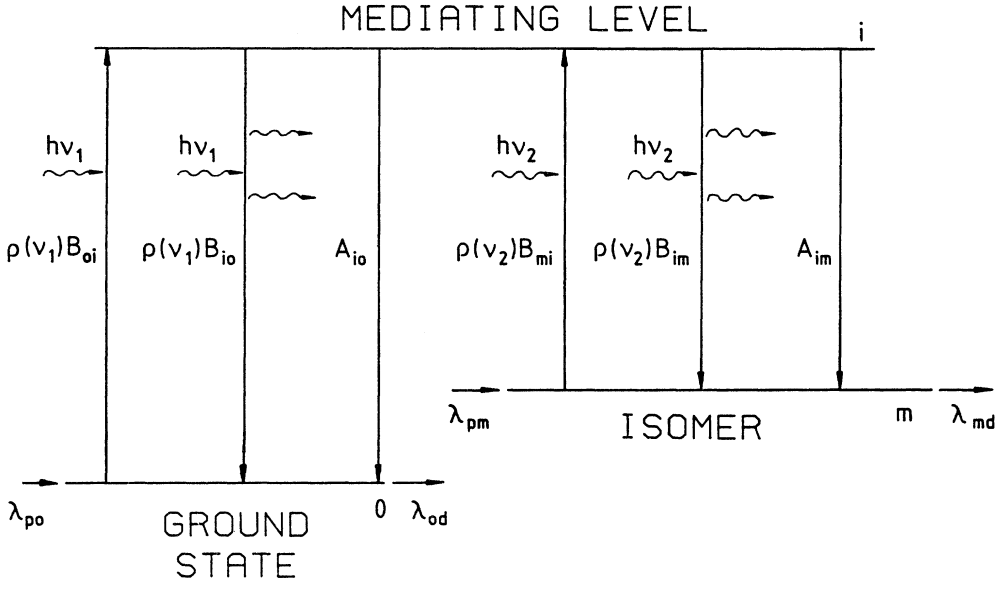


FIG. 2. The possible transitions between ground state and isomer in the presence of a mediating state; direct transitions are forbidden by selection rules.

state exceeds its equilibrium value; the related mean life time $\tau_i$ is given by

$$\tau_i=(A_{i0}+A_{im})^{-1} . \tag{8c}$$

The second solution describes how the populations of the levels $o$ and $m$ approach thermal equilibrium. Defining the branching ratio of the transitions to the isomer as

$$V\equiv A_{im}/(A_{i0}+A_{im}) , \tag{8d}$$

this time constant can be expressed in terms of measurable quantities

$$\lambda_{02}=-\frac{V(1-V)}{\tau_i}\frac{2I_i+1}{2I_m+1}\exp[-(E_i-E_m)/kT] . \tag{9}$$

The larger this rate $\lambda_{02}$, the more efficient is the coupling between ground state and isomer. If more mediating states exist, the corresponding rates can be estimated accordingly. From Eq. (9) one finds that the mediating level with the lowest excitation energy is most important for linking the isomer and the ground state, at least as long as its half-life is sufficiently short.

In the level scheme of $^{176}$Lu, the lowest established mediating level occurs at 838.6 keV. However, this $I^{\pi}=5^-$ state does not decay directly to the isomer but by a cascade that involves other states as well. Therefore, the above approximation has to be extended in order to consider the effect of additional levels.

### C. The time constant of a four-level system

In Fig. 3, the coupling between ground state and isomer involves two higher lying states, $i$ and $k$. From the mediating level $i$ the ground state is reached by a direct transition, while a two step cascade leads to the isomer. The notation is the same as used in the previous example. The population probabilities can be described by a similar set of differential equations making use of the fact, that stimulated emission can be neglected:

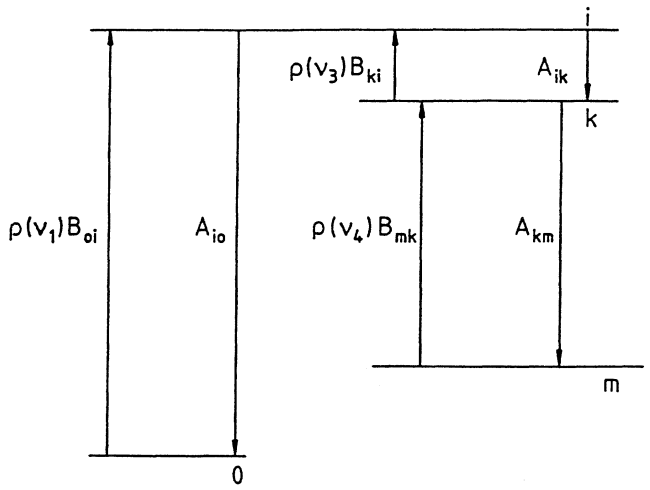


FIG. 3. Transitions in a four level system.

$$\frac{dn_0}{dt}=-\rho B_{oi}n_0+A_{i0}n_i , \tag{10a}$$

$$\frac{dn_i}{dt}=\rho B_{0i}n_0-(A_{i0}+A_{ik})n_i+\rho B_{ki}n_k , \tag{10b}$$

$$\frac{dn_k}{dt}=A_{ik}n_i-(\rho B_{ki}+A_{km})n_k+\rho B_{mk}n_m , \tag{10c}$$

$$\frac{dn_m}{dt}=A_{km}n_k-\rho B_{mk}n_m . \tag{10d}$$

Since the $\rho B$ terms are much smaller than the spontaneous transition probabilities $A$, one obtains a characteristic polynomial

$$P(\lambda)=\lambda(\lambda^3+a\lambda^2+b\lambda+c) \tag{11a}$$

with the coefficients

$$a=A_{i0}+A_{ik}+A_{km} , \tag{11b}$$

$$b=\rho B_{0i}A_{ik}+\rho B_{ki}A_{i0}+A_{km}(A_{ik}+A_{i0}) , \tag{11c}$$

$$c=\rho B_{mk}\rho B_{ki}A_{i0}+\rho B_{0i}A_{km}A_{ik} . \tag{11d}$$

The solutions to this polynomial can be determined analytically, but are rather complex; in particular, they may contain small differences of big numbers, which complicate a reliable treatment. This holds for the numerical solution on a computer as well. Instead, we propose a simple approximation that has been found to work satisfactorily.

We are looking for the smallest eigenvalue $|\lambda_0|\neq 0$, which determines the slowest time dependence of the system. If this solution $\lambda_0$ is sufficiently small, higher order terms in $\lambda$ can be neglected and one obtains

$$\lambda_0=\lambda_a=-\frac{c}{b} . \tag{12a}$$

This result is a good approximation for the true solution if the coefficients of $P(\lambda)$ satisfy the conditions

$$a>\frac{c}{b}=|\lambda_a| , \tag{12b}$$

$$\varepsilon\equiv\frac{ac}{b^2}\ll 1 . \tag{12c}$$

These conditions imply $P(\lambda_a)>0$ and $P(\lambda_a[1+\varepsilon])<0$, so that the maximum error of the approximation is then $\Delta\lambda/\lambda=\varepsilon$. This approximation can be checked by transforming the coefficients into an expression that contains measurable quantities.

$$a=A_i+A_{km} , \tag{13a}$$

$$b=A_iA_{km}+A_i^2V(1-V)\frac{g_i}{g_k}\exp[-(E_i-E_k)/kT] , \tag{13b}$$

$$c=A_i^2A_{km}V(1-V)\frac{g_i}{g_m}\exp[-(E_i-E_m)/kT] . \tag{13c}$$

Here, $A_i=A_{i0}+A_{ik}$ is the inverse lifetime $\tau_i$ of level $i$, $V$ is again the branching factor defined corresponding to

Eq. (8), and $A_{km}$ is the inverse lifetime of the level $k$. It can be shown [21] that both conditions [(12a) and (12b)] are satisfied by these coefficients, so that one obtains finally

$$\lambda_0 = -\frac{A_{km}\, A_i V(1-V)\frac{g_i}{g_m}\exp[-(E_i-E_m)/kT}{A_{km} + A_i V(1-V)\frac{g_i}{g_k}\exp[-(E_i-E_k)/kT]} . \tag{14}$$

Depending on the terms in the denominator, two extreme cases can be distinguished. For sufficiently large transition rates between the intermediate level $k$ and the isomer

$$A_{km} \gg \frac{V(1-V)}{\tau_i}\frac{g_i}{g_k}\exp[-(E_i-E_k)/kT] , \tag{15}$$

one obtains

$$\lambda_0 = -\frac{V(1-V)}{\tau_i}\frac{g_i}{g_m}\exp[-(E_i-E_m)/kT] , \tag{16}$$

identical to the solution for the three-level system. This means that the intermediate state $k$ has no impact as long as it decays rapidly enough to the isomer. The other extreme corresponds to a particularly long life time of level $k$, i.e.,

$$A_{km} \ll \frac{V(1-V)}{\tau_i}\frac{g_i}{g_k}\exp[-(E_i-E_k)/kT] . \tag{17}$$

In this case, the solution

$$\lambda_0 = -A_{km}\frac{g_k}{g_m}\exp[-(E_k-E_m)/kT] \tag{18}$$

implies that the time constant for approaching thermal equilibrium is determined by the half-life of level $k$, the properties of the mediating state $i$ being no longer relevant.

### D. The coupling via the 838.6 keV state

The time constant for approaching thermal equilibrium between ground state and isomer for $^{176}$Lu can now be derived from the completed level scheme. The astrophysically important part of the level scheme (see paper I) with the relevant transitions from the lowest mediating state at 836.6 keV is plotted in Fig. 4. (Weak transitions have been omitted in Fig. 4 for better readability). The decay of the 838.6 keV state is dominated by the direct $E2$ transition to the ground state. Towards the isomer, there is a transition to the $4^-$ bandhead at 722.9 keV, which decays predominantly to a $3^-$ bandhead at 658.5 keV. From there, the gamma cascade includes at least one additional level, but the strongest transitions run across several states.

The half-life of the 658.5 keV level has been measured to $t_{1/2} = 6.5^{+0.3}_{-1.0}$ ns (see paper I, Sec. III E). The 722.9 keV level is also a bandhead, for which a half-life of $\leq 2$ ns was determined. The influence of that level on the time constant $\lambda_0$ needs to be considered, since it acts as the fourth level in Fig. 3. Its decay can be approximated by a direct transition to the isomer at 122.9 keV.

Limits for the half-life of the mediating state at 838.6 keV are available from two experiments: The observation

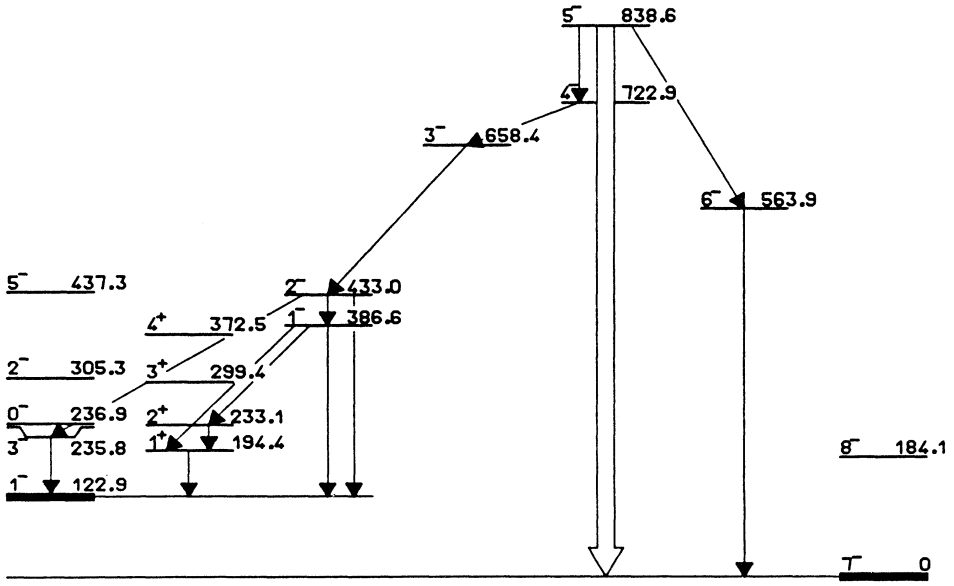


FIG. 4. The relevant part of the level scheme of $^{176}$Lu for the discussion of thermally induced transitions between ground state and the isomer at 123 keV. The $5^-$ state at 838.6 keV, which belongs to the $K^\pi = 4^-$ band, acts as the main mediating level, since it connects the two states by allowed transitions. If $K$-forbidden transitions also contribute; the 437 keV member of the $0^-$ band may be important as well.

of delayed coincidences (paper I, Sec. III E) yields an upper limit of 0.3 ns corresponding to the sensitivity of that technique. A lower limit of $>2.5$ ps can be derived from the line shape of a high resolution measurement with the spectrometer GAMS4 [22], which did not show any Doppler broadening as it is observed for shorter lived states. The branching ratio is determined by the measured gamma intensities in the level scheme (paper I, Table II). However, two of the transitions to the isomer could not be assigned unambiguously. Therefore, the branching factor is found to range between a lower limit $V=0.022$, corresponding to the assumption that only the transition to the bandhead was properly assigned, and an upper limit, $V=0.055$, if the two less well-established transitions are included. Then, one finally obtains

$$7\times10^{7}<\frac{V(1-V)}{\tau_i}<2\times10^{10}\ \mathrm{s}^{-1}\ . \tag{19}$$

At stellar temperatures corresponding to a thermal energy of $kT=25$ keV typical for an *s*-process environment it is

$$\frac{2I_i+1}{2I_k+1}\exp[-(E_i-E_k)/kT]=0.012\ . \tag{20}$$

These experimental results can be used to verify the approximate solutions for the time constant of the four-level system. According to Eq. (15), the 722.9 keV state has negligible influence if it is sufficiently short-lived. The respective limits depend on the assumed half-life of the 838.6 keV state $i$ and are

$$\tau_k \ll 1\ \mu\mathrm{s}\ \text{ for }\ t_{1/2}=0.3\ \text{ns}\ \text{ and }\ kT=25\ \text{keV}\ ,$$

$$\tau_k \ll 7\ \text{ns}\ \text{ for }\ t_{1/2}=2.5\ \text{ps}\ \text{ and }\ kT=25\ \text{keV}\ ,$$

where $\tau_k=A_{km}^{-1}$ is the mean life time of state $k$. Since the measured half-life of the 722.9 keV state is only $\sim3$ times shorter than the 7 ns limit, the second inequality is not strictly valid. However, at the quoted thermal energy of 25 keV, where thermal equilibrium is almost complete, the three-level solution differs only by $\sim20\%$ from the four-level case. With decreasing temperature, the inequality is practically always satisfied. Hence, the three-level solution can be used as a good approximation in the relevant range for *s*-process studies. This means that the scheme of Fig. 2 can further be used for deriving the time constant $\lambda_0$.

In the same way, the influence of all other levels in the decay chain from the 838.6 keV state to the isomer can be investigated. With decreasing excitation energy, these levels can be increasingly long-lived without affecting the validity of the approximation for $\lambda_0$. In particular, this has been verified for the band heads at 658.5 and 194.4 keV with life times of 6.5 and 35 ns. Consequently, the thermal coupling of ground state and isomer under typical *s*-process conditions is exclusively determined by the properties of the 838.6 keV state. Limits for the time constant, by which the closed system approaches equilibrium are obtained by means of the estimates for the life time $\tau_i$ of that level:

$$1.3\times10^{-4}<|\lambda_0|<7\times10^{-3}\ \mathrm{s}^{-1}\ \text{ at }\ kT=25\ \text{keV}\ .$$

This time constant, which describes the effect of internal electromagnetic transitions, is now to be compared with the external production and destruction processes by beta decay and neutron capture.

### E. Neutron capture and beta decay rates

The beta decay rate of the isomer is

$$\lambda_\beta=\ln2/t_{1/2}=5.2\times10^{-5}\ \mathrm{s}^{-1}\ .$$

The neutron capture rate of the ground state depends on the neutron density $n_n$ and can be expressed as

$$\lambda_n=n_n v_T\langle\sigma\rangle\ , \tag{21}$$

where $v_T$ is the mean thermal velocity at temperature $T$, and $\langle\sigma\rangle$ denotes the Maxwellian-averaged neutron capture cross section for the stellar spectrum. With $\sigma=1718\pm85$ mb from Ref. [11] and $n_n=(3.4\pm1.1)\times10^{8}$ cm$^{-3}$ from Ref. [27] one finds

$$\lambda_n=(1.4\pm0.5)\times10^{-7}\ \mathrm{s}^{-1}\approx4\ \mathrm{yr}^{-1}\ .$$

The neutron capture rate of the isomer and the beta decay rate of the ground state can be neglected, since they are much smaller than the respective competing processes.

If the system were closed, it would approach equilibrium with a time constant that, in any event, is not smaller than $|\lambda_0|$. However, at $kT=25$ keV this time scale is much shorter than the inverse neutron capture rate of the ground state, but comparable to the half-life of the isomer. This means that the population probabilities will be affected by temperature. Since the beta decays from the isomer are not negligible, the system is not closed, and *thermal* equilibrium must not be attained necessarily. Instead, a different equilibrium situation will be achieved on a time scale that is large compared to that defined by $|\lambda_0|^{-1}$, provided that the external conditions are stable. This stability could imply constant neutron density and temperature or the repeated *s*-process pulses suggested by stellar models for helium shell burning in AGB stars. In such environments, the equilibrium is determined by the interplay between internal transitions and external production/destruction processes.

### F. The branching factor at equilibrium

The general time dependence upon inclusion of external processes is obtained by solving the differential equations for a three-level system (Fig. 2); the terms for stimulated emission can be neglected for the reason discussed before

$$\frac{dn_0}{dt}=-\rho B_{0i}n_0+A_{i0}n_i-\lambda_{0d}n_0+\lambda_{p0}n_p\ , \tag{22a}$$

$$\frac{dn_i}{dt}=\rho B_{0i}n_0-A_{i0}n_i-A_{im}n_i+\rho B_{mi}n_m\ , \tag{22b}$$

$$\frac{dn_m}{dt}=-\rho B_{mi}n_m+A_{im}n_i-\lambda_{md}n_m+\lambda_{pm}n_p\ . \tag{22c}$$

The equilibrium solution requires $dn/dt=0$, and the re-

sulting system of three linear equations can be solved for $n_m/n_0$:

$$\left[\frac{n_m}{n_0}\right]_{\text{equilib}} = \frac{V\rho B_{0i} + (1-B)\lambda_n}{(1-V)\rho B_{mi} + B\lambda_\beta} . \tag{23}$$

In calculating the ratio of the population probabilities, $n_m/n_0$, the absolute production rate $(\lambda_{pm}+\lambda_{p0})n_p$ cancels out and is replaced by the relative production rate

$$B = \frac{\lambda_{p0}}{\lambda_{p0}+\lambda_{pm}} \quad \text{and} \quad (1-B) = \frac{\lambda_{pm}}{\lambda_{p0}+\lambda_{pm}} . \tag{24}$$

The ratio $B$ corresponds to the partial capture cross section of $^{175}$Lu to the isomer in $^{176}$Lu, which has been remeasured recently for a stellar neutron spectrum with improved accuracy [8] to

$$B = \frac{\sigma^{(g)}}{\sigma_{\text{total}}} = 0.11 \pm 0.04 .$$

This result differs significantly from an older value $B=0.36$ that was used in previous $s$-process analyses [11–13], and is in perfect agreement with the partial cross section at thermal energies, that is deduced from the present level scheme.

With the solution for the equilibrium population of isomer and ground state it is possible to calculate the $s$-process branching factor $f_n$ as well. Since $\lambda_\beta^{(g)} \ll \lambda_n^{(g)}$ and $\lambda_n^{(m)} \ll \lambda_\beta^{(m)}$, Eq. (1) can be rewritten to express $f_n$ as a function of neutron density $n_n$ and temperature $T$:

$$\begin{aligned} f_n^{-1}(n_n,T) &= 1 + \frac{\lambda_\beta^{(m)}}{\lambda_n}\frac{n_m}{n_0} \\ &= 1 + \frac{\lambda_\beta^{(m)}}{\sigma v_T n_n} \frac{V(1-V)\tau_i^{-1}\dfrac{g_i}{g_0}\exp[-E_i/kT] + (1-B)\sigma v_T n_n}{V(1-V)\tau_i^{-1}\dfrac{g_i}{g_m}\exp[-(E_i-E_m)/kT] + B\lambda_\beta^{(m)}} , \end{aligned} \tag{25}$$

which is determined by the properties of the mediating state at 838.6 keV. With the limits for the neutron density derived in Ref. [4], $2.3\times10^8 < n_n < 4.5\times10^8$ cm$^{-3}$, the calculation yields the shaded band in Fig. 5 that can be subdivided into three regions:

(i) At low temperatures, the branching factor is completely determined by the ratio $B$, i.e., by the partial and total neutron capture cross sections of $^{175}$Lu. Induced internal transitions are too weak to have a noticeable effect on the branching.

(ii) Between 200 and 300 million degrees, thermally induced transitions cause drastic changes in the population probabilities of ground state and isomer, leading to significant feeding of the ground state. It is due to this

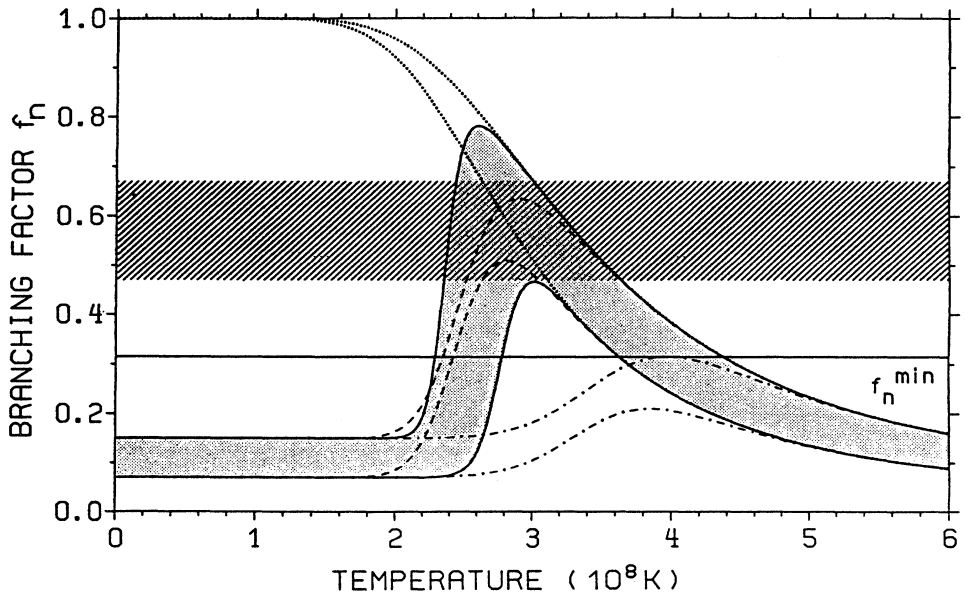


FIG. 5. The branching factor $f_n$ as a function of temperature. The transition between the low temperature regime, characterized by the initial population probabilities due to neutron capture, and the high temperature regime, where complete thermal equilibrium is achieved, occurs at 200 to 300 million degrees (for details see text).

effect that more $^{176}$Lu is observed than would be created in a "cool" environment. In this range, internal transitions, beta decays, and neutron captures are equally important.

(iii) For temperatures higher than 300 million degrees, the relative populations of ground state and isomer correspond to thermal equilibrium, since now the internal transition rates are much larger than those for beta decay or neutron capture.

### G. Comparison with solar abundances

Knowing the temperature dependence of the branching factor $f_n$, the observed $^{176}$Lu abundance can be discussed in terms of a chronometer or a thermometer for the $s$ process. At first, a clear lower limit for $f_n$ can be estimated from the observed solar abundances of $^{176}$Lu and $^{176}$Hf via Eq. (1):

$$f_n \geq \frac{\langle\sigma\rangle N(^{176}\text{Lu})}{\langle\sigma\rangle N(^{176}\text{Lu})+\langle\sigma\rangle N(^{176}\text{Hf})} \ . \tag{26}$$

Here, $N$ denotes the abundances produced during the $s$ process. Until now, the abundance of $^{176}$Lu has decreased by radioactive decay, and this fraction of decayed $^{176}$Lu represents the relevant input parameter for a determination of the $s$-process age.

In turn, this fraction can be constrained by comparison with the age of the solar system. The $s$ process being definitely older than the solar system yields

$$N(^{176}\text{Lu}) \geq N_{\odot}\exp[\lambda_{\beta} t_{\text{sol}}] \ ,$$

where $t_{\text{sol}}=4.6\times10^9$ yr is the age of the solar system, and $N_{\odot}$ is today's $^{176}$Lu abundance. The ratio of the solar element abundances of Lu and Hf has been determined rather accurately to $N_{\odot}(\text{Lu})/N_{\odot}(\text{Hf})=0.243\pm0.008$ [11]. This implies an isotopic $s$-process abundance of

$$N(^{176}\text{Lu})/N(^{176}\text{Hf}) \geq 0.138$$

at the formation of the solar system, if a 3% correction for a possible $p$-process contribution to the $^{176}$Hf abundance is allowed for. With the cross section ratio $\langle\sigma\rangle(^{176}\text{Lu})/\langle\sigma\rangle(^{176}\text{Hf})=3.32$, one obtains eventually a lower limit for the branching factor

$$f_n^{\min}=0.31 \ .$$

This value is included in Fig. 5 to demonstrate that the observed $^{176}$Lu abundance definitely *requires* thermal effects to operate during the $s$ process. In the region, where $f_n$ is independent of temperature, the small partial cross section to the ground state would result in an underproduction of $^{176}$Lu by at least a factor of 2 compared to its observed abundance.

The onset of thermally induced transitions between isomer and ground starts first by transforming part of the $^{176}$Lu$^m$ population to the ground state before it can beta decay. In this way, the $^{176}$Lu abundance increases with temperature until the photon bath is hot enough to compensate for the different energy steps from the isomer and the ground state to the mediating level. In that limit, thermal equilibrium is established, which can be described by Eq. (4) with $n_m/n_0=(g_m/g_0)\exp[-E_m/kT]$:

$$f_n=\frac{\lambda_n^{(0)}+\frac{g_m}{g_0}\exp[-E_m/kT]\lambda_n^{(m)}}{\lambda_n^{(0)}+\frac{g_m}{g_0}\exp[-E_m/kT](\lambda_n^{(m)}+\lambda_{\beta}^{(0)})} \ . \tag{27}$$

For the hypothetical case, that thermal equilibrium would prevail already at low temperatures, Eq. (27) shows $f_n$ approaches unity as $T$ drops to zero (dotted lines in Fig. 5); this solution would greatly overproduce $^{176}$Lu$^g$ while $^{176}$Hf would be bypassed in the $s$-process neutron capture chain.

To summarize this important point it is to be stressed that the initially high population of $^{176}$Lu$^m$, as it results from the neutron capture reaction, is strongly reduced at sufficiently high temperatures. Above ~200 million degrees, the stellar photon bath becomes energetic enough to change the initial populations towards thermal equilibrium between ground state and isomer via the mediating level at 838.6 keV; this results in a sharp rise for the population of the ground state, and hence of the branching factor, $f_n$. If thermal equilibrium is fully established, the population probability of the isomer rises with increasing temperature, and the branching factor decreases again.

Consequently, there is a certain temperature range, where just the right amount of $^{176}$Lu$^g$ is produced to account for the presently observed abundance. With the lower limit for $f_n$ determined above, $^{176}$Lu can be interpreted as a sensitive thermometer: Fig. 5 shows immediately that the allowed temperature for the $s$-process ranges from $2.4\times10^8$ to $4.4\times10^8$ K.

### H. The branching factor from $s$-process systematics

The temperature limits for the $s$ process can be restricted further by deducing the branching factor $f_n$ from the description of the $\sigma N(A)$ curve via the so-called classical approach. In the framework of this model, a formal solution for $f_n$ has been given by Beer *et al.* [11], which is presented on the basis of the input data discussed above.

The entire $s$-process flow through mass 176 is given by

$$f(A)=(\langle\sigma\rangle N)_{176}=\langle\sigma\rangle N(^{176}\text{Lu})+\langle\sigma\rangle N(^{176}\text{Hf}) \ . \tag{28}$$

Starting at $t=0$ from *today's* solar abundances $N_{\odot}$ the actual abundances produced in the $s$ process are obtained by means of the radioactive decay law. Going backwards in time, the abundances were

$$N_{\text{Lu}}(t)=N_{\text{Lu},\odot}\exp[\lambda t]$$

and

$$N_{\text{Hf}}(t)=N_{\text{Hf},\odot}-(\exp[\lambda t]-1)N_{\text{Lu},\odot} \ . \tag{29}$$

In this discussion, the indices Lu and Hf denote always $^{176}$Lu and $^{176}$Hf, respectively. Since $f(A)$ is known from systematic studies [4], Eqs. (28) and (29) can be solved for $[\lambda t]$:

$$\exp[\lambda t]=\frac{f(A)-\langle\sigma\rangle_{\rm Hf}(N_{\rm Hf,\odot}+N_{\rm Lu,\odot})}{(\langle\sigma\rangle_{\rm Lu}-\langle\sigma\rangle_{\rm Hf})N_{\rm Lu,\odot}} \ . \tag{30}$$

Obviously, it is important for deducing $[\lambda t]$ that $^{176}$Lu and $^{176}$Hf do have different stellar cross sections, so that a characteristic abundance pattern in the $A=176$ branching can evolve. The branching factor can be expressed by Eq. (30)

$$f_n=\frac{\langle\sigma\rangle_{\rm Lu}N_{\rm Lu,\odot}\exp[\lambda t]}{f(A)} =\frac{\dfrac{1-\langle\sigma\rangle_{\rm Hf}(N_{\rm Hf,\odot}+N_{\rm Lu,\odot})}{f(A)}}{1-\dfrac{\langle\sigma\rangle_{\rm Hf}}{\langle\sigma\rangle_{\rm Lu}}} \ . \tag{31}$$

The experimental input data for calculating $f_n$ are the cross sections at $kT=30$ keV. $\sigma_{\rm Lu}=1537\pm60$ mb and $\sigma_{\rm Hf}=458\pm20$ mb [11,23,24] as well as the observed solar abundances, $N_{\rm Lu,\odot}=0.000984\pm1.3\%$ and $N_{\rm Hf,\odot}=0.00802\pm1.9\%$ [10]. Adopting the value for $f(A)=(\langle\sigma\rangle N)_{176}=7.08\pm0.38$ at $kT=30$ keV from Ref. [4], one obtains the branching factor including the uncertainties of all input data:

$$f_n=0.57\pm0.10 \ .$$

This result is given in Fig. 5 as the hatched band; from its overlap with the band for $f_n(T)$, the possible range for the $s$-process temperature reduces to

$$2.4\times10^8\le T\le3.6\times10^8 \ \text{K} \ .$$

### I. $^{176}$Lu as a chronometer

Since the branching at $A=176$ has been found to depend crucially on temperature, it is certainly very difficult to answer the question of a further interpretation of $^{176}$Lu as a chronometer. This is best illustrated by solving Eq. (30) for the beta decay rate of the $^{176}$Lu ground state, which yields an $s$-process age

$$44\times10^8\le t\le61\times10^9 \ \text{yr} \ .$$

The evident discrepancy between this result and other determinations of cosmic ages can only be explained by assuming that the decay of $^{176}$Lu was accelerated for some time, possibly even after its production in the $s$ process. The respective temperature dependence of the $^{176}$Lu half-life can now be calculated on the basis of the completed level scheme.

### J. The temperature dependence of the beta decay rate

In the absence of neutrons, the beta decay of $^{176}$Lu can be described again by means of the three-level system of Fig. 2. After termination of the neutron exposure, there is no more production of $^{176}$Lu ($\lambda_{p0}=\lambda_{pm}=0$), and destruction occurs only by beta decay ($\lambda_{0d}=\lambda_\beta^{(0)}$; $\lambda_{md}=\lambda_\beta^{(m)}$). Because of the beta decay, the populations of ground state and isomer exhibit a continuous decrease that can be described by the differential equations (22a)–(22c) with the above modifications, using the ansatz $n_x(t)=c_x\exp(\lambda t)$ with $x=0,m,i$. The solution for the ground state decay [21] is

$$n_0(t)=N_{\rm Lu}\exp(-\lambda_0 t) \ , \tag{32}$$

where the beta decay rate of $^{176}$Lu, $\lambda_0$ includes the effect of thermal couplings between ground state and isomer,

$$\lambda_0(T)=\frac{(A_{i0}+A_{im})\lambda_\beta^{(m)}\lambda_\beta^{(g)}+A_{i0}A_{im}\left[\dfrac{g_m}{g_0}\exp(-E_i/kT)\lambda_\beta^{(m)}+\dfrac{g_i}{g_m}\exp[-(E_i-E_m)/kT]\lambda_\beta^{(g)}\right]}{(A_{i0}+A_{im})\lambda_\beta^{(m)}+A_{i0}A_{mi}\dfrac{g_i}{g_m}\exp[-(E_i-E_m)/kT]} \ . \tag{33}$$

From this expression for $\lambda_0(T)$, two extreme cases can be distinguished. First, for very low temperatures one obtains the beta decay rate of the ground state, $\lambda_0=\lambda_\beta^{(g)}$, since thermal effects can still be neglected. Second, at very high temperatures, Eq. (33) reduces to

$$\lambda_0(T)=\lambda_\beta^{(m)}\frac{g_m}{g_0}\exp(-E_m/kT) \ . \tag{34}$$

In this case, thermal equilibrium is attained and the internal couplings are much faster than beta decay from the isomer.

For the astrophysical discussion it is now very important that thermal equilibrium is reached only at a certain temperature. Thus, how equilibrium is approached depends again on the properties of the mediating state. With the experimental life time limits for the level at 838.6 keV, one arrives at the temperature dependence of the $^{176}$Lu half-life plotted in Fig. 6 as the shaded band. Note the extremely sharp decrease of $t_{1/2}$ over 10 orders of magnitude that is completely determined by the limits for the lifetime $\tau_i$. Presumably, this pronounced temperature dependence makes $^{176}$Lu a sensitive probe for the temperature profile and the time scale for dredge-up of freshly synthesized material from the stellar $s$-process site to cooler zones in the convective envelope.

Figure 6 also contains this case, if there were a fast direct transition between isomer ground state. Then, thermal equilibrium would always be complete, and the half-life would be reduced already at much lower temperatures (dotted line). The indirect coupling via the 838.6

keV state bears, therefore, important consequences for the stability of $^{176}$Lu at high temperatures.

### K. The influence of *K* forbidden transitions

So far, all calculations were only based on the mediating state at 838.6 keV. The influence of the next mediator at 921.5 keV is already much smaller due to its higher excitation energy, since the lifetime of this level is similar to that of the 838.6 keV state (paper I, Sec. III E). This appears plausible, since the two states differ neither in their spins and $K$ quantum numbers nor in their decay systematics. Hence, among the well-established mediating levels, the 838.6 keV state certainly dominates the thermal effects in $^{176}$Lu.

For a thorough discussion, two remaining questions have to be addressed. First, the level scheme may contain an *undetected* mediating level at lower excitation energy, which could give rise to an enhanced thermal coupling. The comparison with model calculations has demonstrated, however, that the present scheme can be considered to be complete for levels of intermediate spin up to 900 keV. Second, the branching ratio $V$ for one of the *known* levels may be so small that only the strongest transition in one of the partial level schemes was found, but that a mediating transition fell below the sensitivity limit of the spectrometer. Such transitions from one of the lower lying states would be $K$ forbidden, and their possible influence must be considered in more detail.

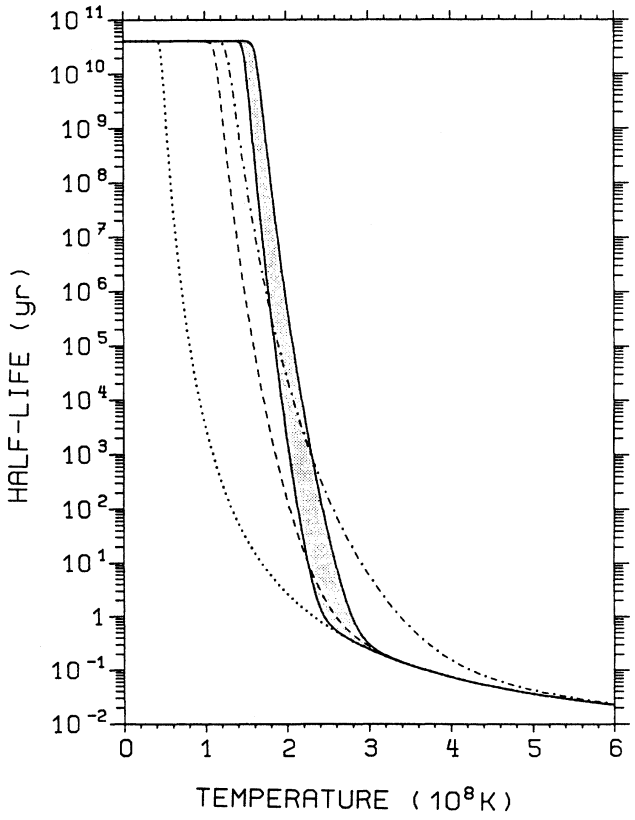


FIG. 6. The temperature dependence of the $^{176}$Lu half-life.

A rough calculation using Weisskopf estimates [25] for the transition rates in combination with $K$-hindrance factors, $\delta = 10^{-2|\Delta K - L|}$, shows that the $5^-$ member (at 437 keV) of the $K^\pi = 0^-$ band (Fig. 4) would provide the most efficient connection between ground state and isomer; however, it also shows that the effect of all $K$-forbidden transitions is considerably smaller than the coupling via the 838.6 keV level. The influence of these transitions is indicated in Figs. 5 and 6 by dashed-dotted lines. Obviously, the resulting branching factor $f_n$ would be too small to account for the observed $^{176}$Lu abundance (Fig. 5). As far as the half-life of $^{176}$Lu is concerned (Fig. 6), one finds an effect already at somewhat lower temperatures, but the $K$-allowed transitions take over long before the beta-decay half-life has reached the typical time scale for neutron captures of $\sim 0.1$ yr.

However, experimental $E2$ intraband transitions are often orders of magnitude larger than the Weisskopf estimates. This fact is confirmed by the measured $E2/M1$ mixing ratios in $^{176}$Lu. For example, comparison of a known $E2$ contribution in the $K=0$ band with the Weisskopf estimates for $M1$ and $E2$ transitions yields an $E2$ enhancement of $\sim 600$. Also the energy dependence for the $E2$ rates differs from the $E_\gamma^5$ slope predicted by the Weisskopf estimate. This is illustrated by the observation that the well-defined $E2/M1$ ratios in a $K^\pi = 1^+$ band are energy-independent. Since the expected $E_\gamma^3$ dependence for $M1$ transitions is experimentally verified by observed branching ratios, the collective $E2$ intraband transitions obviously exhibit the same $E_\gamma^3$ dependence.

A modified empirical estimate for the rate of the $K$-forbidden 437.3 keV $E2$ transition from the above mentioned $5^-$ member to the ground state was determined by multiplying the Weisskopf rate for a $M1$ transition with the $E2/M1$ mixing ratio measured in the $K=0$ band; in this way, one obtains an enhancement factor of $\sim 200$. If this modified rate is again scaled with the $K$-hindrance factor $\delta$, one now finds that the $K$-forbidden transitions are almost as efficient in thermalizing $^{176}$Lu as the allowed transitions via the 838.5 keV state (dashed lines in Figs. 5 and 6). In the relevant temperature range, however, the thermal effects are still dominated by $K$-allowed transitions, since they determine the beta decay half-life whenever it falls low enough that competition with $(n,\gamma)$ reactions becomes important.

The two estimates for the rate of the ground state transition from the 437 keV level may be considered as lower and upper bounds, both indicating a rather small influence of that level. The systematics of $K$-forbidden transitions [26] does also not suggest a considerably smaller $K$-hindrance than the adopted factor, $\delta = 10^{-2|\Delta K - L|}$. Hence, it appears most likely that the thermally induced equilibration between ground state and isomer in $^{176}$Lu is, indeed, dominated by allowed transitions via the 838.6 keV state.

## III. CONCLUSIONS

The thermal enhancement of the beta decay rate of $^{176}$Lu and its consequences for the stellar production of that isotope could be discussed quantitatively on the basis

of detailed experimental information of the level scheme. It was found that the thermal coupling of ground state and isomer in $^{176}$Lu is determined by only two levels: (i) an $I^{\pi}=5^{-}$, $K=4$ state at 838.6 keV, for which the mediating transitions were found experimentally, and (ii) an $I^{\pi}=5^{-}$, $K=0$ state at 437.3 keV. The influence of the second state depends strongly on the assumption for the rate of its $K$-forbidden ground state transition. With an improved estimate based on observed $E2/M1$ mixing ratios one finds that the second level may also contribute significantly to the thermal coupling. However, the thermal effects appear likely to be dominated by allowed transitions via the 838.6 keV state, at least in the temperature range of interest for the $s$ process.

As a consequence of the coupling between ground state and isomer, the $s$-process production of $^{176}$Lu becomes a sensitive function of temperature. Competition between beta decays and neutron captures at $^{176}$Lu results in an $s$-process branching that can, for the first time, be described quantitatively. It is found that its original abundance is determined by the neutron densities and temperatures at the $s$-process site, and remains, therefore, too uncertain for using $^{176}$Lu as a chronometer for the age of the $s$-process. Instead, it can rather be considered as a suitable $s$-process thermometer, yielding a temperature range between $2.4\times10^{8}$ and $3.6\times10^{8}$ K, in good agreement with similar estimates from other $s$-process branchings and with current stellar models [27].

*Present address: Asea Brown Boveri, Corporate Research, CH-5405 Baden, Switzerland.

[1] R. J. Gehrke, C. Casey, and R. K. Murray, Phys. Rev. C **41**, 2878 (1990), and references therein.
[2] J. Audouze, W. A. Fowler, and D. N. Schramm, Nature **238**, 8 (1972).
[3] M. Arnould, Astron. Astrophys. **22**, 311 (1973).
[4] F. Käppeler, H. Beer, and K. Wisshak, Rep. Prog. Phys. **52**, 945 (1989).
[5] B. J. Allen, G. C. Lowenthal, and J. R. de Laeter, J. Phys. G **7**, 1271 (1981).
[6] B. J. Allen, G. C. Lowenthal, J. W. Boldeman, and J. R. de Laeter, in *Neutron Capture Gamma-Ray Spectroscopy and Related Topics,* edited by T. von Egidy, F. Gönnenwein, and B. Maier (Institute of Physics, Bristol, 1982), p. 573.
[7] F. Stecher-Rasmussen, K. Abrahams, J. Kopecky, J. Lindner, and P. Polak, P., in *Capture Gamma-Ray Spectroscopy 1987,* edited by K. Abrahams and P. Van Assche (Institute of Physics, Bristol, 1988), p. 754.
[8] W. R. Zhao and F. Käppeler, in *Astrophysical Ages and Dating Methods,* edited by J. Audouze, M. Cassé, and E. Vangioni-Flam (Editions Frontières, Gif-sur-Yvette, 1989), p. 357; Phys. Rev. C **44**, 506 (1991).
[9] H. Beer and F. Käppeler, Phys. Rev. C **21**, 534 (1980).
[10] E. Anders and N. Grevesse, Geochim. Cosmochim. Acta **53**, 197 (1989).
[11] H. Beer, G. Walter, R. L. Macklin, and P. J. Patchett, Phys. Rev. C **30**, 464 (1984).
[12] R. A. Ward (private communication).
[13] H. Beer, F. Käppeler, K. Wisshak, and R. A. Ward, Astrophys. J. Suppl. **46**, 295 (1981).
[14] A. Veres and I. Pavlicsek, Acta Phys. Acad. Sci. Hung. **28**, 419 (1970).
[15] E. B. Norman and S. Kellogg, Astrophys. J. **291**, 834 (1985).
[16] L. Lakosi, I. Pavlicsek, and A. Veres, in *Capture Gamma-Ray Spectroscopy 1987,* edited by K. Abrahams and P. Van Assche (Institute of Physics, Bristol, 1988), p. S745.
[17] D. G. Gardner, M. A. Gardner, and R. W. Hoff, in *Capture Gamma-Ray Spectroscopy 1987,* edited by K. Abrahams and P. Van Assche (Institute of Physics, Bristol, 1988), p. S315; J. Phys. G (Suppl.) **14**, S315 (1988).
[18] Y. Watanabe, T. Mukoyama, and S. Shimizu, Phys. Rev. C **23**, 695 (1981).
[19] F. Käppeler, in *Capture Gamma-Ray Spectroscopy 1987,* edited by K. Abrahams and P. Van Assche (Institute of Physics, Bristol, 1988), p. S297; J. Phys. G (Suppl.) **14**, S297 (1988).
[20] R. A. Ward and W. A. Fowler, Astrophys. J. **238**, 266 (1980).
[21] N. Klay, Kernforschungszentrum Karlsruhe Report KfK-4675 (1990).
[22] H. G. Börner, private communication (1990).
[23] Z. Y. Bao and F. Käppeler, At. Data Nucl. Data Tables **36**, 411 (1987).
[24] W. Ratynski and F. Käppeler, Phys. Rev. C **37**, 595 (1988).
[25] C. M. Lederer and V. S. Shirley, *Table of Isotopes* (Wiley, New York, 1978).
[26] K. E. G. Löbner, Phys. Lett. **26B**, 369 (1968).
[27] F. Käppeler, R. Gallino, M. Busso, G. Picchio, and C. M. Raiteri, Astrophys. J. **354**, 630 (1990).